Fully paired-configuration mixing calculations in ^{46}Ti and ^{48}Cr

Y. Han
Department of Physics, Sichuan University, Chengdu 610064, People's Republic of China
(Received 29 July 1999; published 19 May 2000)

The basic theoretical formalism of angular momentum projection based on a particle-number-conserving treatment is elaborated. This method is, for the first time, applied to the middle of the *fp* shell. Full paired-configuration mixing calculations in the even-even deformed nuclei ^{46}Ti and ^{48}Cr show that only small parts (weight>0.01) of the configuration components are important for the case of either ground states or excited states. Low-lying excited energy spectra and reduced transition probabilities $B(E2)$ in the $K=0$ bands can be reproduced well only by admixing very limited fully paired configurations. The improvements in the energy spectra are much more prominent than those without configuration mixing. The calculated $B(E2)$ values are more reasonable in comparison with the available experimental data, as well as those from other models.

PACS number(s): 21.10.Re, 21.60.−n, 27.40.+z

I. INTRODUCTION

During the last three decades, the shell-model configuration mixing (SCM) calculations have yielded extremely valuable contributions to the microscopic understanding of many nuclear structure properties. However, it is well known that the SCM approach is restricted to rather small model spaces or comparable basis systems due to the very large dimensions of the matrices that need to be diagonalized. Recent technological innovations have extended the shell-model calculations up to $A\approx 60$ region [1], where the energy spectra and other properties of nuclei can be studied by exact diagonalizations in a full major oscillator shell. Because of the much larger configuration space required, the heavier nuclei (for example, those of the rare-earth region) cannot be studied by using this procedure yet. Even if it may technically be attainable on a modern supercomputer, such a calculation is not of much interest from a physical point of view, because it is very difficult to guarantee that the data obtained in this way are able to uncover the physics hidden behind a vast amount of computer output [2].

In order to overcome the above-mentioned and some other drawbacks [2,3] in the SCM calculations, many approaches have been developed and extensively applied to investigate the structure of various nuclei both in low- and high-spin states, such as the deformed configuration mixing (DCM) [4–7] calculations based on the angular momentum projection of the deformed Hartree-Fock intrinsic states [8], the projection theory of Hartree-Fock-Bogoliubov (HFB) intrinsic states [9–12], and the projected shell model (PSM) [2] based on the angular momentum and particle-number projection of the quasiparticle states in the Nilsson plus BCS representation, etc. Undoubtedly, these methods have achieved great success in describing the energy spectra, the electromagnetic properties, and some other important structure phenomena of nuclei. Among the above approximate treatments, both the PSM and HFB methods are based on the BCS theory. Generally speaking, using BCS theory to treat the problems of the nuclear pairing correlation is considered to be suitable for a system containing a large number of particles, but in a nucleus where the number of the valence particles which dominate the behavior of low-lying states is very small, nonconservation of particle number may lead to some serious troubles, such as the occurrence of excessive spurious states in the low-lying excited spectra, orthogonality, blocking effects, etc. [13–18]. According to such an analysis, Zeng *et al.* [13–18] proposed a particle-number-conserving (PNC) scheme, in which all the difficulties encountered in the BCS theory disappeared. The PNC method has been successfully used to investigate many nuclear structure problems [13–18]. However, the PNC wave functions have no definite angular momentum, and the rotational symmetry is violated. In order to restore the symmetry and to compare directly with experimental data, the angular momentum projections of the PNC wave functions have to be performed so that the nuclear states with good angular momenta can be obtained.

One of the purposes of this paper is to present an angular momentum projection method in the framework of the PNC treatment, and the basic theoretical formalism of the angular momentum projection of the PNC wave functions (PPNC) is given in Sec. II. The other purpose is to check the feasibility of the present projection theory by practical calculations. As the first application of this method, we calculate the low-lying excited energy spectra and reduced transition probabilities $B(E2)$ in the $K=0$ bands for the deformed even-even nuclei ^{46}Ti and ^{48}Cr in the full *fp* model space since the data from the other theories and recent experiments about these two nuclei are relatively plentiful. The details of the calculations, the comparisons with other models, and the corresponding discussions are given in Sec. III. It needs to be emphasized that the configuration mixing calculations presented in this paper only include the fully paired configurations to describe nuclear low-lying energy spectra and properties. In order to reproduce the higher excited spectra and properties of nuclei (such as ''the backbending anomaly''), it is necessary to consider the pair-broken effects. However, is it enough only to add the pair-broken configurations into the configuration mixing for exactly showing the pair-broken effects? More detailed discussions relating to this problem are given in the subsection ''Broken pairs and cranking frequency'' in Sec. III. In Sec. IV, we make a summary of this work.

II. THEORETICAL FORMALISM

For an axially symmetric deformed nucleus, the pairing Hamiltonian is usually expressed as

$$H=\sum_{\mu>0}\varepsilon_\mu(a_\mu^\dagger a_\mu+a_{\bar{\mu}}^\dagger a_{\bar{\mu}})-G\sum_{\xi,\mu>0}a_\xi^\dagger a_{\bar{\xi}}^\dagger a_{\bar{\mu}}a_\mu, \quad (1)$$

where μ is the single-particle state, $\bar{\mu}$ is the time-reversal state of μ, ε_μ is the single-particle energy, and G is the average strength of nuclear pairing interaction. The states μ and $\bar{\mu}$ are twofold degenerate. One eigenfunction (i.e., the PNC wave function) of H can be expressed as [13–18]

$$|\Psi_\nu\rangle=\sum_\sigma w_{\nu\sigma}|\Phi_\sigma\rangle, \quad (2)$$

where $|\Phi_\sigma\rangle$ is an intrinsic state (Slater determinant), which is constructed from a set of the appropriate deformed single-particle states and corresponds to a configuration σ obtained by distributing the nucleons over these single-particle states. $\nu=0$ indicates the ground state, and $\nu=1,2,\ldots,$ indicate the excited states. $w_{\upsilon\sigma}$ are the expanding coefficients, satisfying the normalization condition

$$\sum_\sigma w_{\nu\sigma}^2=1. \quad (3)$$

Obviously, the PNC wave functions given in Eq. (2) have no definite total angular momentum I and only have good quantum number K and parity π. Using the angular momentum projection operator $\hat{P}^I_{MK}$ to act upon the PNC wave function $|\Psi_\nu\rangle$, we can make a linear superposition

$$|\Xi_{aIM}\rangle=\sum_\nu F_{\alpha\nu_I}\hat{P}^I_{MK}|\Psi_\nu\rangle. \quad (4)$$

The projection operator is given by [8]

$$\hat{P}^I_{MK}=\frac{2I+1}{8\pi^2}\int D^I_{MK}(\Omega)^*\hat{R}(\Omega)d\Omega, \quad (5)$$

where $D^I_{MK}(\Omega)$ is the D function, $\hat{R}(\Omega)=e^{-i\alpha J_x}e^{-i\theta J_y}e^{-i\gamma J_z}$ is the three-dimensional rotational operator, Ω represents a set of Euler angles $(\alpha,\theta=[0,\pi],\ \gamma=[0,2\pi])$, and the J's are the angular momentum operators.

Let the coefficients $F_{\alpha\nu I}$ in Eq. (4) satisfy the normalization condition

$$\langle\Xi_{aIM}|\Xi_{aIM}\rangle=\sum_{\nu'\nu}F_{\alpha\nu' I}N^I_{\nu'\nu}F_{\alpha\nu I}=1, \quad (6)$$

where

$$N^I_{\nu'\nu}\equiv\langle\Psi_{\nu'}|\hat{P}^I_{K'K}|\Psi_\nu\rangle=\left(I+\frac{1}{2}\right)\sum_{\sigma'\sigma}w_{\nu'\sigma'}w_{\nu\sigma}\times\int_0^\pi\langle\Phi_{\sigma'}|e^{-i\theta J_y}|\Phi_\sigma\rangle d^I_{K'K}(\theta)\sin(\theta)d\theta, \quad (7)$$

here $d^I_{K'K}(\theta)$ is the d function. Then the nuclear energies with good angular momentum I should be

$$E_{aI}=\langle\Xi_{aIM}|H|\Xi_{aIM}\rangle=\sum_{\nu'\nu}F_{\alpha\nu' I}H^I_{\nu'\nu}F_{\alpha\nu I}, \quad (8)$$

where

$$H^I_{\nu',\nu}\equiv\langle\Psi_{\nu'}|H\hat{P}^I_{K'K}|\Psi_\nu\rangle=\left(I+\frac{1}{2}\right)\sum_{\sigma'\sigma}w_{\nu'\sigma'}w_{\nu\sigma}\times\int_0^\pi\langle\Phi_{\sigma'}|He^{-i\theta J_y}|\Phi_\sigma\rangle d^I_{K'K}(\theta)\sin(\theta)d\theta. \quad (9)$$

The matrix element of a tensor operator of rank λ can be evaluated by using

$$\langle\Xi_{a'I'M'}|\hat{T}_{\lambda\mu}|\Xi_{aIM}\rangle=(IM\lambda\mu|I'M')\langle\Xi_{a'I'}\|\hat{T}_\lambda\|\Xi_{\alpha I}\rangle=(IM\lambda\mu|I'M')\sum_{\kappa\nu'\nu}F_{a'\nu'I'}F_{a\nu I}\times(I,K'-\kappa,\lambda\kappa|I'K')\sum_{\sigma'\sigma}w_{\nu'\sigma'}w_{\nu\sigma}\times\langle\Phi_{\sigma'}|\hat{T}_{\lambda\kappa}\hat{P}^I_{K'-\kappa,K}|\Phi_\sigma\rangle, \quad (10)$$

where $(IM\lambda\mu|I'M')$, etc. are the Clebsch-Gordon coefficients.

For the fully paired configurations ($K=0$ and seniority $\upsilon=0$) of an even-even nucleus with $n/2$ pairs of valence nucleons, the intrinsic states $|\Phi_\sigma\rangle$ are invariant under the time-reversal transformation. Therefore, Eq. (8) can reduce to

$$E_{\nu,I,K=0}=\frac{\Sigma_{\sigma'\sigma}w_{\nu\sigma'}w_{\nu\sigma}\int_0^{\pi/2}H_{\sigma'\sigma}(\theta)d^I_{00}(\theta)\sin(\theta)d\theta}{\Sigma_{\sigma'\sigma}w_{\nu\sigma'}w_{\nu\sigma}\int_0^{\pi/2}N_{\sigma'\sigma}(\theta)d^I_{00}(\theta)\sin(\theta)d\theta},$$
$$I=0,2,4,\ldots,I_{\max}, \quad (11)$$

where

$$N_{\sigma'\sigma}(\theta)=\langle\Phi_{\sigma'}|e^{-i\theta J_y}|\Phi_\sigma\rangle, H_{\sigma'\sigma}(\theta)=\langle\Phi_{\sigma'}|He^{-i\theta J_y}|\Phi_\sigma\rangle, \quad (12)$$

in which $J_y=\Sigma_i j_y(\mathbf{r}(i))$, and $\mathbf{r}(i)$ stands for the radius vector of the ith nucleon. Equation (10) reduces to

$$\langle \Xi_{\nu' I' M'} | \hat{T}_{\lambda\mu} | \Xi_{\nu I M} \rangle = (IM\lambda\mu | I' M') \langle \Xi_{\nu' I'} \| \hat{T}_{\lambda} \| \Xi_{\nu I} \rangle$$
$$= (IM\lambda\mu | I' M') (N^{I'}_{\nu'\nu'} N^{I}_{\nu\nu})^{-1/2}$$
$$\times \sum_{\kappa} (I, -\kappa, \lambda\kappa | I' 0)$$
$$\times \sum_{\sigma' \sigma} w_{\nu'\sigma'} w_{\nu\sigma} \langle \Phi_{\sigma'} | \hat{T}_{\lambda\kappa} \hat{P}^{I}_{-\kappa,0} | \Phi_{\sigma} \rangle, \tag{13}$$

where

$$N^{I}_{\nu\nu} = (2I+1) \sum_{\sigma' \sigma} w_{\nu\sigma'} w_{\nu\sigma} \int_0^{\pi/2} N_{\sigma'\sigma}(\theta) d^{I}_{00}(\theta) \sin(\theta) d\theta. \tag{14}$$

In calculating the various electromagnetic moments and transition probabilities, the tensor operator $\hat{T}_{\lambda\mu}$ in Eq. (13) should have different forms. For the reduced transition probability $B(E2)$, the operator $\hat{T}_{\lambda\mu}$ can be taken as [8]

$$\hat{T}^{E}_{2\mu} = \frac{1}{2} \sum_{i=1}^{n} [(1+\tau_3(i)) e_p + (1-\tau_3(i)) e_n] r^2(i) Y_{2\mu}(i), \tag{15}$$

where $\tau_3(i)$ is twice the z component of isospin of the ith nucleon, e_p and e_n are the effective charges for protons and neutrons, respectively. The $B(E2)$ value can be evaluated by

$$B(E2; I \to I') = \frac{2I'+1}{2I+1} |\langle \Xi_{\nu' I'} \| \hat{T}^{E}_{2} \| \Xi_{\nu I} \rangle|^2. \tag{16}$$

If only the fully paired configuration ($K=0$) mixing is considered, the projected energy spectrum for a certain nucleus can be calculated with Eqs. (11) and (12), and various electromagnetic properties can be obtained by using Eqs. (13) and (14). In the following section, Eqs. (11)–(16) will be used to calculate the energy spectra and $B(E2)$ values for the even-even nuclei ^{46}Ti and ^{48}Cr in the *fp* shell, and some discussions will be presented in detail.

III. CALCULATIONS AND DISCUSSIONS

In this work, the single-particle states are chosen in the following way to construct the intrinsic states $|\Phi_{\sigma}\rangle$, which are assumed to be suitable for the nuclei ^{46}Ti and ^{48}Cr. We take ^{40}Ca as an inert core and restrict ourselves in the full *fp* model space including the four single-particle orbits $1f_{7/2}$, $1f_{5/2}$, $2p_{3/2}$, and $2p_{1/2}$ to obtain the deformed Hartree-Fock (HF) single-particle states. In the deformed HF self-consistent calculations, the modified surface delta interaction (MSDI) [19] is used due to its mathematical simplicity and its success in accounting for many nuclear properties. The MSDI reads [20]

$$v^{MSDI}(1,2) = -4\pi A'_T \delta(\mathbf{r}(1) - \mathbf{r}(2)) \delta(r(1) - R_0) + B' \tau(1) \cdot \tau(2) + C', \tag{17}$$

where $\mathbf{r}(1)$ and $\mathbf{r}(2)$ are position vectors of interacting particles, and R_0 is the nuclear radius, T in A'_T is total isospin quantum number, A'_1 and A'_0 stand for the strength parameters of $T=1$ and 0, respectively. $A_T = A'_T f(R_0)$, $B = B' f(R_0)$, $C = C' f(R_0)$, and $f(R_0)$ is a positive number relating to R_0 or mass number A. For the parameters A_T, B, and C, there is an empirical estimate [20]

$$A_1 \approx A_0 \approx B \approx 25 \ \text{MeV}/A, C \approx 0. \tag{18}$$

In a set of basis functions $|nljm\tau\rangle$, which may be taken to be the eigenstates of the spherical harmonic-oscillator Hamiltonian and be abbreviated as $|jm\tau\rangle$, a deformed HF single-particle state $|i\rangle$ can be expanded as

$$|i\rangle = \sum_{j} C_{jm_i\tau_i} |jm_i\tau_i\rangle. \tag{19}$$

In the representation $|jm\tau\rangle$ the matrix elements of the single-particle Hamiltonian h should be expressed as

$$\langle j'm\tau | h | jm\tau \rangle = e_{j'j} \delta_{j'j} + \sum_{i=1}^{n} \sum_{j_1 j_2} C_{j_1 m_i \tau_i} C_{j_2 m_i \tau_i} \times \langle j'm\tau, j_1 m_i \tau_i | v_{\text{anti}} | jm\tau, j_2 m_i \tau_i \rangle, \tag{20}$$

where $\delta_{j'j}$ is the Kronecker δ symbol, e_j are a set of single-particle energies of the spherical shell model, n is the number of valence nucleons outside the core, and the subscript of v_{anti} indicates that the matrix elements of the two-body interaction are antisymmetrized. More details of the deformed HF self-consistent calculation can be found in the literature (see, for example, Ref. [21]).

A. Energy spectra and $B(E2)$ values in ^{46}Ti

1. Single-particle states

After carrying out the deformed HF self-consistent calculations for ^{46}Ti, we can obtain the single-particle energies and wave functions (listed in Table I) of the lowest energy configuration that is called the HF ground-state configuration. Figure 1(a) shows the scheme of the single-particle orbits occupied and unoccupied by neutrons and protons for the HF ground-state configuration of ^{46}Ti. This configuration is taken as the reference state and is called the $0p$(particle)-$0h$(hole) state, while the other configurations are considered to be the *p-h* excited states. The single-particle energies and wave functions of these *p-h* excited states can be obtained from different variational procedures. By comparing with the phenomenological Nilsson single-particle scheme, it can be known that the HF ground-state configuration is a prolate state. Our calculations show that those *p-h* excited states with relatively low energies are also prolate. The projection of the total spin on the intrinsic symmetry axis is $K = \sum_{i=1}^{n} m_i$. For each fully paired configuration, there is $K=0$. In this work, the values of the spherical single-particle

TABLE I. The deformed HF single-particle energies ε_i (in MeV) and wave functions of the HF ground-state configuration for ^{46}Ti. In the present HF calculations, protons and neutrons are undistinguished so the isospin subscripts τ_i of the coefficients $C_{jm_i\tau_i}$ have been omitted. In order to identify the different single-particle states with the same magnetic quantum numbers, we use $|m_i|$ with a numerical subscript to denote the single-particle orbit i in the first column.

Orbits i	ε_i	$C_{7/2m_i}$	$C_{5/2m_i}$	$C_{3/2m_i}$	$C_{1/2m_i}$
$1/2_1$	−12.967	0.767	−0.219	−0.546	0.258
$1/2_2$	−4.162	0.010	0.686	0.055	0.726
$1/2_3$	−8.294	0.622	0.422	0.501	−0.429
$1/2_4$	−6.260	0.160	−0.551	0.669	0.472
$3/2_1$	−10.345	0.965	0.122	−0.234	0
$3/2_2$	−4.194	−0.085	0.983	0.162	0
$3/2_3$	−6.829	0.250	−0.136	0.958	0
$5/2_1$	−8.870	0.999	−0.034	0	0
$5/2_2$	−3.194	0.034	0.999	0	0
$7/2_1$	−8.390	1.0	0	0	0

energies $e_{7/2}$, $e_{5/2}$, $e_{3/2}$, and $e_{1/2}$ in Eq. (20) are taken from experiment [22], which are −8.36, −2.86, −6.29, and −4.32 MeV, respectively. For ^{46}Ti, considering the empirical estimate, Eq. (18), we select a group of MSDI strength parameters that can make the projected energy spectrum agree well with the experimental energy spectrum. A_1, A_0, B, and C are 0.50, 0.37, 0.35, and 0.05 MeV, respectively.

2. Pure configuration-projected energy spectrum

We first calculate the projected energy spectrum from the angular momentum projection without configuration mixing

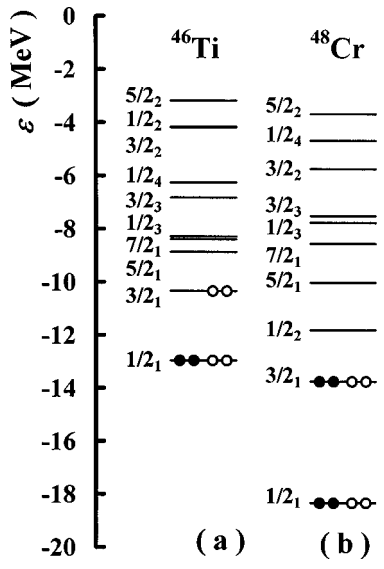

FIG. 1. The deformed HF single-particle energy level schemes of the HF ground-state configurations for ^{46}Ti and ^{48}Cr. ε stands for the single-particle energy. The dots represent the protons, the circles represent the neutrons. See Table I for the details of the orbits.

TABLE II. The fully paired configurations used in the angular momentum projection calculations for ^{46}Ti and ^{48}Cr, σ stands for the configuration number. The details of the configurations are listed in the last column, e.g., the configuration $2p(\nu 5/2_1)^2-2h(\nu 3/2_1)^2$ denotes a $2p-2h$ fully paired configuration, which is formed by exciting a pair of neutrons from the orbit $3/2_1$ into the orbit $5/2_1$ in the $0p-0h$ state (reference state, which is the HF ground-state configuration). See text and Fig. 1.

Nuclei	σ	Configurations p (particle), h (hole), π (proton), ν (neutron)
^{46}Ti	1	$0p-0h$
	2	$2p(\nu 5/2_1)^2-2h(\nu 3/2_1)^2$
	3	$2p(\nu 3/2_1)^2-2h(\nu 1/2_1)^2$
^{48}Cr	1	$0p-0h$
	2	$2p(\nu 1/2_2)^2-2h(\nu 3/2_1)^2$
	3	$2p(\nu 5/2_1)^2-2h(\nu 3/2_1)^2$
	4	$4p(\nu 1/2_2)^2(\pi 1/2_2)^2-4h(\nu 3/2_1)^2(\pi 3/2_1)^2$
	5	$4p(\nu 5/2_1)^2(\pi 5/2_1)^2-4h(\nu 3/2_1)^2(\pi 3/2_1)^2$

(i.e., the pure configuration projection [8,23]). The three intrinsic states corresponding to the configurations $\sigma=1,2,3$ (see Table II) are constructed with the deformed HF single-particle states from three different variational procedures, respectively. The three corresponding projected rotational bands are labeled as A', B', and C' in Fig. 2, respectively.

3. Fully paired configuration mixing energy spectrum

In the PNC treatment, Eq. (2) requires the intrinsic state set $\{|\Phi_\sigma\rangle\}$ to be a set of the complete basis. However, the different HF intrinsic states are from the different variational procedures so that they may not be orthogonal to each other. This problem may be solved by carrying out an orthogonalizing procedure. Considering the fact that the different groups of single-particle wave functions from the different variational procedures are numerically very close to each other for ^{46}Ti, we make such an approximate treatment to simplify the operations: all the intrinsic states $|\Phi_\sigma\rangle$ are constructed by using a set of fixed single-particle states, which can be taken from the variational procedure corresponding to the HF ground-state configuration. Obviously, the intrinsic states constructed in such a way are orthogonal to each other.

As mentioned above, the single-particle scheme of the HF ground-state configuration is used to construct all the intrinsic states (Slater determinants). If the configuration energy truncation is not adopted, the number of such intrinsic states is obviously very large. However, our calculations show that very limited p-h excited states may be sufficient to provide an adequate description of the low-lying states of the nuclei. In the following configuration mixing calculations for obtaining the low-lying energy levels in $K=0$ bands of ^{46}Ti, only the three lowest energy prolate fully paired configurations are used. They are the $0p$-$0h$ state (reference state) and

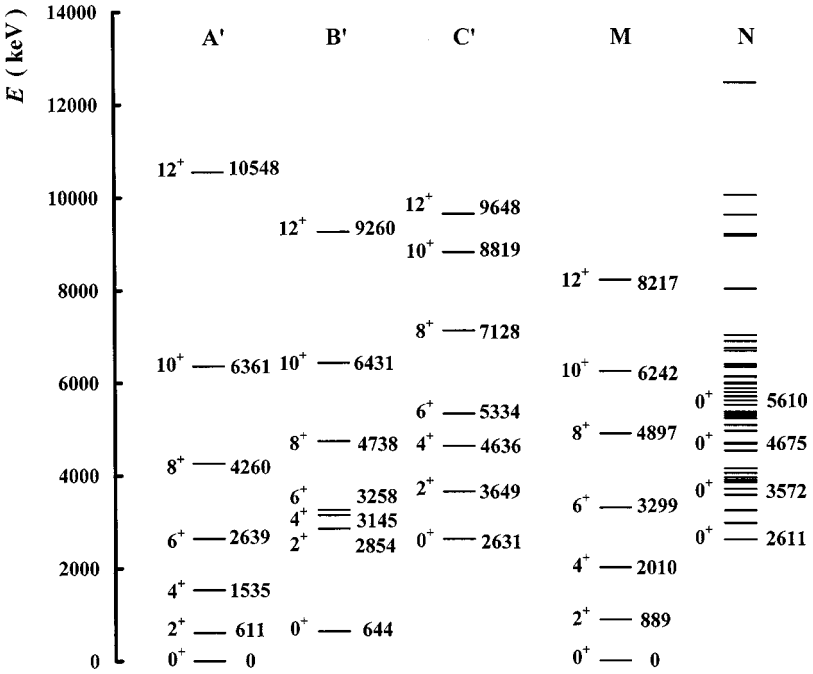

FIG. 2. The experimental [24,25] and the pure configuration-projected energy spectra of ^{46}Ti. A', B', and C' are three rotational bands from the angular momentum projections of the three intrinsic states corresponding to the three paired configurations (see Table II for the details). M is the yrast band from experimental data, and N denotes the other experimental energy levels, where only the energy values of the excited 0^+ states are marked.

the two lowest $2p$-$2h$ states (one has a pair of excited neutrons, the other has a pair of excited protons; see Table II). The three corresponding intrinsic states are marked as $\Phi_{\sigma=1,2,3}$, respectively.

Figure 3 shows the plots of eight angular momentum-projected matrix elements versus the Euler θ. It can be verified easily that, in the range $[0, \pi]$, each of the projected matrix elements $N_{\sigma'\sigma}(\theta)$ [or $H_{\sigma'\sigma}(\theta)$] is symmetrical about the straight line $\theta=\pi/2$ due to the time-reversal invariant qualities of the fully paired configurations. Therefore, the curves of the eight projected matrix elements only in the range $[0, \pi/2]$ are given in Fig. 3. As seen in this figure, the absolute values of the diagonal elements decrease rapidly approaching to zero with θ increasing when the values of θ values are close to a certain value $\theta=\theta_0$, for example, $\theta_0 \approx \pi/4$ for $N_{11}(\theta)$ [or $H_{11}(\theta)$]. The absolute value of the off-diagonal element is relatively smaller, and a peak appears between $\theta=0$ and $\theta=\pi/2$. For example, the peak of $N_{11}(\theta)$ [or $H_{11}(\theta)$] is at the point $\theta\approx 7\pi/60$. In the previous works on the pure configuration projection calculations [8,23], all these off-diagonal matrix elements were neglected. However, since the number of zero points of $d^I_{K'K}(\theta)$ in Eq. (11) increases as I increases, only considering the diagonal matrix elements is not very reasonable although the magnitudes of these diagonal elements are much greater than those of the off-diagonal elements.

The average pairing interaction strength G, in principle, can be experimentally determined by the even-odd mass difference [13]. In the calculations for ^{46}Ti, the value of G is 0.55 MeV. By diagonalizing the Hamiltonian H in the space spanned by the three lowest energy fully paired configurations, we obtain the eigenvalues E_ν and the PNC wave func-

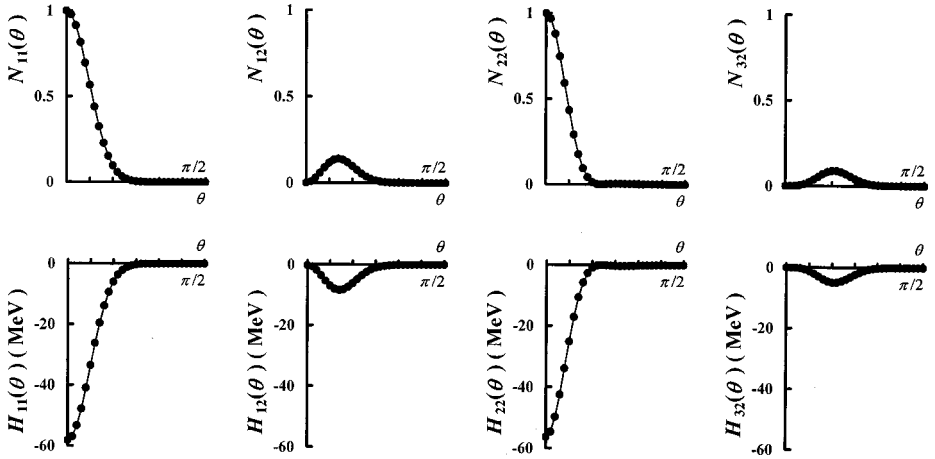

FIG. 3. The plots of the angular-momentum-projected matrix elements $N_{\sigma'\sigma}(\theta)$ and $H_{\sigma'\sigma}(\theta)$ versus the Euler angle θ for ^{46}Ti. For each matrix element, the 30 points are calculated. See Table II for the details of the configurations numbered by σ.

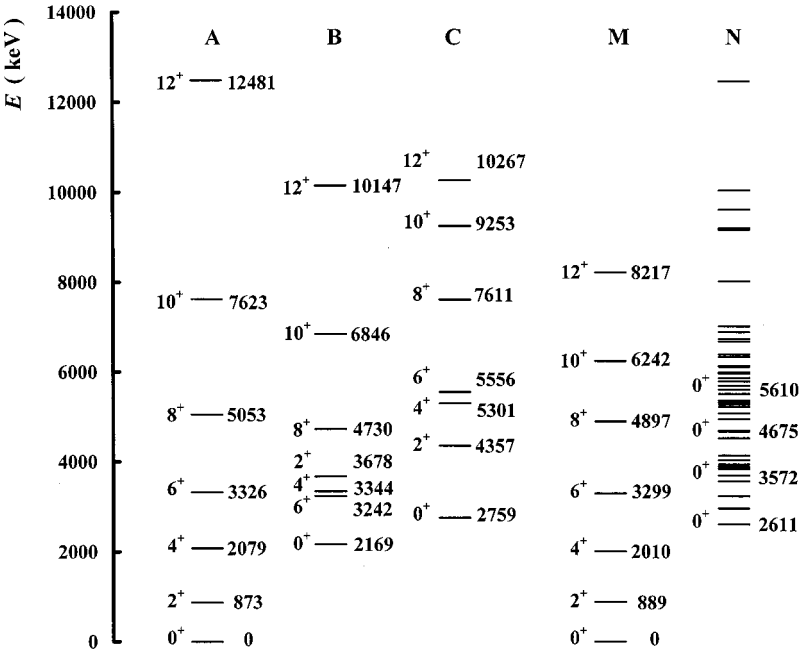

FIG. 4. The experimental [24,25] and the fully paired configuration mixing energy spectra for ^{46}Ti. *M* is the yrast band from experimental data, and *N* denotes the other experimental energy levels, where only the energy values of the excited 0^+ states are marked. The fully paired configuration mixing spectrum consists of the rotational bands *A*, *B*, and *C*, which are from the angular momentum projections of the three PNC wave functions. See the text for the details of the three PNC wave functions.

tions. For the ground state ($\nu=0$), there is

$$E_0=-74.4 \text{ MeV},$$
$$|\Psi_0\rangle=0.9798|\Phi_1\rangle+0.1735|\Phi_2\rangle+0.0999|\Phi_3\rangle; \tag{21}$$

for the excited states ($\nu=1,2$), there are

$$E_1=-71.2 \text{ MeV},$$
$$|\Psi_1\rangle=-0.1700|\Phi_1\rangle+0.9845|\Phi_2\rangle-0.0426|\Phi_3\rangle, \tag{22}$$

$$E_2=-68.9 \text{ MeV},$$
$$|\Psi_2\rangle=-0.1057|\Phi_1\rangle+0.0247|\Phi_2\rangle+0.9941|\Phi_3\rangle. \tag{23}$$

As seen from Eq. (21), the $\sigma=1$ configuration ($0p$-$0h$ prolate state) with the largest weight is the most important component of the ground state. In the pure configuration projection, $\sigma=1$ configuration is directly regarded as the nuclear ground state, and the corresponding projected rotational band is referred to as the ''ground-state band'' [8,23]. The situation of excited states is analogous with this. From such a point of view, it can be said that the pure configuration projection is only a special case of the PPNC calculation, where all the off-diagonal angular momentum-projected matrix elements are neglected, and equivalently the average pairing interaction strength *G* is taken to be 0.

Using Eq. (11) the projected spectrum is obtained from the PNC wave functions $|\Psi_{\nu=0,1,2}\rangle$, which consist of three rotational bands *A*, *B*, and *C* as shown in Fig. 4. In Figs. 2 and 4, *M* denotes the experimental yrast band [24,25]. In the projected ground-state band *A*, the levels $I^\pi=2^+-8^+$ are nearly coincident with those in band *M*, while the levels $I^\pi=2^+-8^+$ in band A' (as shown in Fig. 2) from the pure configuration projections have a larger difference than the experimental ones. The 0^+ levels in the bands *B* and *C* in Fig. 4 agree with the experimental data much better than those in bands B' and C' in Fig. 2. In band B', the levels 2^+, 4^+, and 6^+ are very close and are going up in order. In band *B*, these levels have also very close energies, but they are going down in order due to the configuration mixing. However, due to the larger space between levels in band C', the order of levels after mixing (band *C*) is not inverted. For the higher-spin states in the excited bands, it is difficult to compare the calculated results with experiment due to the scarcity of experimental data.

4. Broken pairs and cranking frequency

In the above-mentioned calculations for the low-lying excited spectrum of ^{46}Ti, we have made a configuration energy truncation [truncated energy $E_c=E_2=-68.9$ MeV in Eq. (23)] after the *K* truncation (only the three $K=0$ configurations are considered). The 2^+-8^+ levels in band *A* (see Fig. 4) are very coincident with those in the experimental yrast band, but the observed backbending spin states above level 8^+ in the yrast band is not reproduced well by the present calculations, in which only fully paired configurations were used. The pair-broken effects may be important for the high-spin states in the yrast band. Therefore, the configuration mixing may need to include the pair-broken configurations (seniority $v=2,4,6,...$, and generally $K\neq 0$) when I^π is 10^+ (or larger) in the case of ^{46}Ti. Consequently, the configuration mixing not including the broken pairs will result in a larger discrepancy between the experiments and calculations for the states above the level 8^+ in the yrast band. For this reason, the ''ground-state band'' *A* (see Fig. 4) from the fully paired configuration mixing calculations cannot be seen as the ''realistic'' yrast band, especially for the states at and above the backbending point.

TABLE III. The $B(E2)$ values in the ground-state band of ^{46}Ti. Their units are e^2 fm^4. Exp. is the experiment [25–27]; Th.1 is PPNC; Th.2 is the projection of the pure HF ground-state configuration; Th.3 is MONSTER [28]; Th.4 is the $(f_{7/2})^6$ shell mode [27]; Th.5 is the rotational mode [27]. In our calculations (Th.1 and Th.2), the pure $E2$ transition limit is assumed.

$I_i^\pi \to I_f^\pi$	Exp.	Th.1	Th.2	Th.3	Th.4	Th.5
$2^+ \to 0^+$	180 ± 8[a]	132	134	138	116	215
	190 ± 10[b]					
	215 ± 20[c]					
$4^+ \to 2^+$	206 ± 39[c]	186	184	186	127	304
$6^+ \to 4^+$	147 ± 29[c]	196	188	189	110	342
$8^+ \to 6^+$	108 ± 20[c]	183	175	172	122	352
$10^+ \to 8^+$	117 ± 29[c]	143	157	119	69	362
$12^+ \to 10^+$	29 ± 3[c]	56	124	51	41	372

[a]Reference [25].
[b]Reference [26].
[c]Reference [27].

As has been stated, the K mixture (triaxiality), in which all the configurations including the pair-broken configurations are admixed, should be considered so as to reproduce the observed backbending spin states. However, since the time-reversal invariance of the corresponding intrinsic states disappears in $K \neq 0$ configurations, Eqs. (10) and (13) cannot be used any longer in the K mixture. Thus, Eq. (6) needs to be solved exactly for evaluating the normalization coefficients $F_{\alpha\nu I}$ in Eq. (4).

In the cranked-shell model, the average nuclear potential is considered to rotate at a cranking frequency ω, about the x axis perpendicular to the symmetry z axis. The effect of the Coriolis interaction $H_c = -\omega J_x$, where operator J_x is the projection of the total spin on the x axis, has not been introduced in our calculations, namely, the condition of $\omega = 0$ has been assumed for the low-lying states. For the higher-spin states in the yrast band, this effect cannot be neglected. Using the particle-number-conserving treatment in the cranked-shell model, Wu and Zeng [15,16] have performed many calculations and shown that the components of $v = 2$ and 4 are mixed gradually into yrast states with increasing cranking frequency ω. When $\omega \geqslant \omega_c$, where ω_c is a critical frequency, the yrast state will undergo a great change, the component of fully paired configurations ($v = 0$, $K = 0$) decreases below 50%, the component of one-pair-broken configurations ($v = 2$) increase up to 40%, and the component of two-pair-broken configurations ($v = 4$) becomes non-negligible ($\approx$10%), while that of $v \geqslant 6$ configurations is still negligibly small. These results clearly display the close relationship among the broken pairs, the cranking frequency ω, and the yrast states. Therefore, in order to show the pair-broken effects exactly, only taking the pair-broken configurations into account in the mixing calculations is not enough. It may be more essential and significant to introduce a cranking term (Coriolis interaction) $-\omega J_x$ into the Hamiltonian given by Eq. (1). Furthermore, if the cranking term is introduced, the K is no longer a good quantum number. This makes the angular momentum projection matrix elements more complicated.

TABLE IV. The eigenvalues E_ν (in MeV) and the expanding coefficients $\omega_{\nu\sigma}$ corresponding to the five PNC wave functions $\Psi_{\nu=0,1,2,3,4}$ for ^{48}Cr.

ν	E_ν	$\omega_{\nu 1}$	$\omega_{\nu 2}$	$\omega_{\nu 3}$	$\omega_{\nu 4}$	$\omega_{\nu 5}$
0	−131.11	0.9794	0.1757	0.0987	0.0144	0.0043
1	−127.14	−0.1884	0.9593	0.1381	0.1585	0.0081
2	−123.41	−0.0727	−0.0986	0.9386	−0.3117	0.0825
3	−123.07	−0.0074	−0.1978	0.2874	0.9368	0.0265
4	−115.97	0.0036	0.0049	−0.0869	−0.0004	0.9962

From the above discussions, it seems that (1) the calculated ''yrast band'' is likely to be closer to the observed (''realistic'') yrast band if the pair-broken configurations and the cranking term $-\omega J_x$ are simultaneously considered; (2) in the yrast band of a nucleus, the nuclear shape will undergo a change from axial symmetry to triaxiality when spin I is up to the critical value I_c.

5. B(E2) values in ground-state band

To test the wave functions, we calculate the reduced transition probability $B(E2)$ of ^{46}Ti. Most of the available experimental data [25–27] are in the yrast band. Therefore, we only calculate the $B(E2)$ values in the ground-state band for

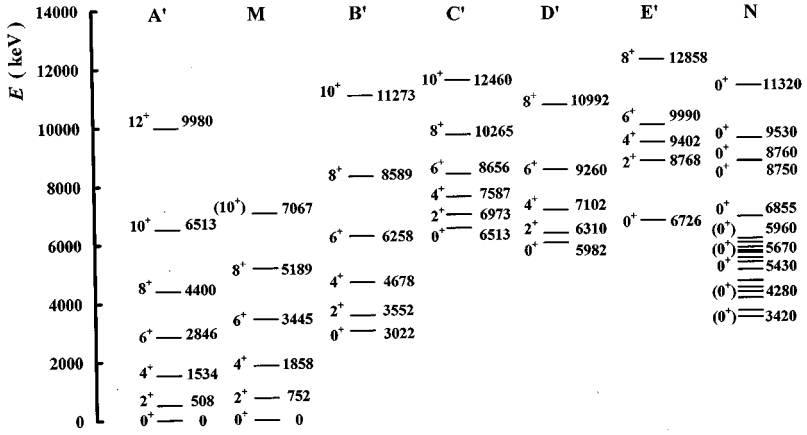

FIG. 5. The experimental [29,30] and the pure configuration-projected energy spectra for ^{48}Cr. A', B', C', D', and E' are five rotational bands from the angular momentum projections of the five intrinsic states corresponding to the five fully paired configurations (see Table II for the details). M is the yrast band from experimental data, and N denotes other experimental energy levels, where only the energy values of the excited 0^+ states are marked.

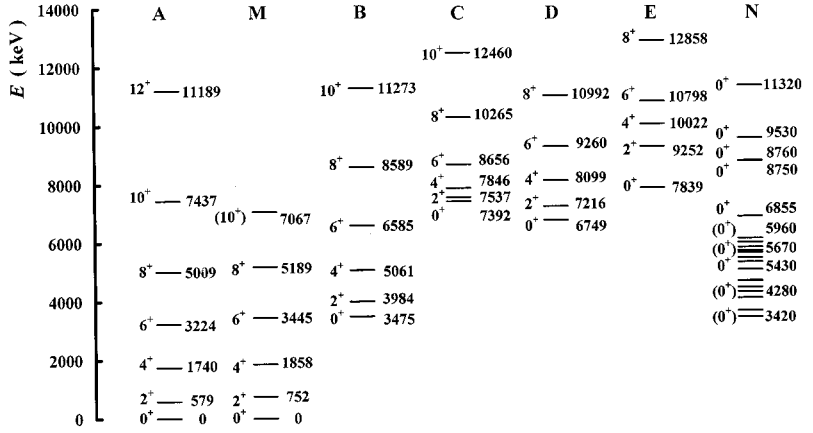

FIG. 6. The experimental [29,30] and the fully paired configuration mixing energy spectra for ^{48}Cr. *M* is the yrast band from experimental data, and *N* denotes other experimental energy levels, where only the energy values of the excited 0^+ states are marked. The fully paired configuration mixing spectrum consists of the rotational bands *A*, *B*, *C*, *D*, and *E*, which are from the angular momentum projections of five PNC wave functions. See the text for the details of the five PNC wave functions.

comparing them with the experimental ones conveniently. Our results and those from other models are listed in Table III. In our calculations (Th.1 and Th.2, see Table III), the effective proton charge e_p is taken as $1.83e$, and let the effective neutron charge e_n satisfy the relation of $e_p - e = 0.83e$. It is $e_p = e_n = 0.7e$ in Th.3 (MONSTER [28]) and $e_p = e_n = 0.9e$ in Th.4 [the $(f_{7/2})^6$ shell model [27]]. As seen from Table III, the $B(E2)$ values of every model except for Th.5 (the rotational model [27]) do follow the trend of experimental data. The $B(E2)$ values calculated by Th.1, Th.2, and Th.3 are almost the same for the transitions below the 8^+ states. However, the $B(E2;10^+ \rightarrow 8^+)$ and $B(E2;12^+ \rightarrow 10^+)$ values calculated by Th.1 and Th.3 are more consistent with the experimental data than those calculated by Th.2 due to the configuration mixing.

B. Energy spectra and $B(E2)$ values in ^{48}Cr

1. Single-particle states and PNC wave functions

For ^{48}Cr, we use the five fully paired configurations (see Table II) to span the configuration space. Figure 1(b) shows the deformed HF ground-state single-particle level scheme, which is used to construct the five intrinsic states corresponding to the five configurations. For the spherical single-particle energies $e_{7/2}$, $e_{5/2}$, $e_{3/2}$, and $e_{1/2}$, the same values as ^{46}Ti are used. Considering the differences in nuclear radius R_0 between ^{48}Cr and ^{46}Ti, the MSDI strength parameters A_1 and A_0 are changed to 0.75 and 0.65 MeV, respectively. The values of *B* and *C* (0.35 and 0.05 MeV, respectively) are fixed for the two nuclei ^{46}Ti and ^{48}Cr. The parameter *G* is taken as 0.65 MeV.

The eigenvalues E_ν and the expanding coefficients $w_{\nu\sigma}$ corresponding to the PNC wave functions $\Psi_{\nu=0,1,2,3,4}$ are listed in Table IV. It can be seen that the weight of the configuration $\sigma=5$ is already very small (<0.01) for the ground state ($\nu=0$). Therefore, those configurations, in which the excited nucleons are distributed over the orbits far from the Fermi surface, may be not necessary to be considered in the configuration mixing calculations. Thus by selecting the important configurations (generally taking the weight>0.01), the computing time can be greatly reduced while a sufficient degree of accuracy can be kept. The cases of the excited states ($\nu=1,2,...$) are similar to that of the ground state.

2. Low-lying levels in K=0 bands

Figure 5 shows the experimental [29,30] and the pure configuration projection energy spectra. The five intrinsic states corresponding to the configurations $\sigma=1,2,3,4,5$ (see Table II) are constructed with the deformed HF single-particle states from the five different variational procedures, respectively. The five corresponding projected rotational bands are marked as A', B', C', D', and E' in Fig. 5, respectively. Figure 6 shows the energy spectra from the experiments and the PPNC method. The mixed rotational bands are marked as *A*, *B*, *C*, *D*, and *E* corresponding to $\nu=0$ (ground state), 1, 2, 3, 4 (excited states), respectively. As seen from Figs. 5 and 6, $I^\pi = 0^+ - 10^+$ levels in band *A* reproduce those of the experimental yrast band *M* much better than band A'. As to the excited bands, the experimental data are scarce and we do not intend to discuss them here.

3. B(E2) values in ground-state band

For the $B(E2)$ values of ^{48}Cr, the available experimental data [26,30] are still mainly in the yrast band and have great uncertainty. We only show those $B(E2)$ values within the ground-state band. Our result (Th.1 and Th.2), the result (Th.3) obtained by Caurier *et al.* [1] using the full *pf* shell model, and the experimental data (Exp.) are listed in Table V. In our calculations, the effective charges e_p and e_n, taken to be the same as those of ^{46}Ti, are $1.83e$ and $0.83e$, respectively. It can be seen from Table V that the $B(E2)$ values calculated by the PPNC method are of a reasonable agreement in comparison with the experimental data and those of Th.3. The result of Th.1 is slightly better than those (Th.2) from the pure configuration projection, so the $B(E2)$ values in the ground-state band for ^{48}Cr are not so sensitive to the fully paired configuration mixing as ^{46}Ti.

IV. SUMMARY

In the framework of particle-number-conserving (PNC) treatment, we apply the angular momentum projection techniques to the even-even deformed nuclei ^{46}Ti and ^{48}Cr in the

TABLE V. The $B(E2)$ values in the ground-state band of ^{48}Cr. Their units are $e^2\,\mathrm{fm}^4$. Exp. is the experiment [26,30]. Th.1 is PPNC; Th.2 is the projection of the pure HF ground-state configuration; Th.3 is the full *pf* shell model [1]. In our calculations (Th.1 and Th.2), the pure $E2$ transition limit is assumed.

$I_i^\pi \to I_f^\pi$	Exp.	Th.1	Th.2	Th.3
$2^+ \to 0^+$	321 ± 41[a]	204	205	228
	266 ± 40[b]			
$4^+ \to 2^+$	259 ± 83[a]	271	271	312
$6^+ \to 4^+$	>155[a]	265	264	311
$8^+ \to 6^+$	67 ± 23[a]	239	241	285
$10^+ \to 8^+$	>35[a]	230	236	201
$12^+ \to 10^+$		200	209	146

[a]Reference [30].
[b]Reference [26].

fp shell. Full paired-configuration mixing calculations show that the components of the relatively important configurations (weight$>$0.01) are very limited for the nuclear ground state or excited states, so that the configuration space can be truncated to be very small. Well-reproduced low-lying excited energy spectra and reduced transition probabilities $B(E2)$ in the $K=0$ bands can be obtained only by admixing a few fully paired configurations. The improvements in the energy spectra are much clearer than those without configuration mixing. The calculated $B(E2)$ values are more reasonable in comparison with the available experimental data as well as those from other models.

It is well known that exact treatment of the blocking effects in BCS formalism is very difficult. However, it is very easy to take the blocking effects into account exactly by using the PNC treatment [13,14]. One of the developing aims of the PPNC method presented in this paper is to apply it to study both the low- and higher-spin states of various (even-even, odd-*A*, and odd-odd) nuclei with the consideration of the pair-broken effects. Therein, the blocking effects are automatically taken into account. The other aim is, by using the different single-particle scheme appropriate for them in the different regions of nuclei, to extend this projection method to study the heavier nuclei, where the SCM calculations have not already been performed. Moreover, some shortcomings (as mentioned in Sec. I), which are encountered due to the particle-number nonconservation of wave functions in the BCS theory, do not exist in the PPNC formalism. Therefore, we have reason to believe that the present method is more advantageous.

ACKNOWLEDGMENTS

The author is very grateful to Professor J. Z. Liao for his continuous support during this work. The author would like to express his sincere thanks to Professor J. Y. Zeng, Professor C. S. Wu, and Dr. Y. A. Lei for their encouragement and help. The author also thanks Dr. M. Gong and Dr. C. L. Yang for some interesting discussions.

[1] E. Caurier, A. P. Zuker, A. Poves, and G. Martinez-Pinedo, Phys. Rev. C **50**, 225 (1994).
[2] K. Hara and Y. Sun, Int. J. Mod. Phys. E **4**, 637 (1995).
[3] K. W. Schmid, F. Grummer, and A. Faessler, Phys. Rev. C **29**, 291 (1984).
[4] A. K. Dhar, D. R. Kulkarni, and K. H. Bhatt, Nucl. Phys. **A238**, 340 (1975); A. K. Dhar and K. H. Bhatt, *ibid.* **A271**, 36 (1976).
[5] R. Sahu and S. P. Pandya, Nucl. Phys. **A529**, 20 (1991); **A548**, 64 (1992); **A571**, 253 (1994).
[6] A. K. Rath, C. R. Praharaj, and S. D. Khadkikar, Phys. Rev. C **47**, 1990 (1993).
[7] S. Chattopadhyay, H. C. Jain, and M. L. Jhingan, Phys. Rev. C **50**, 93 (1994).
[8] C. S. Warke and M. R. Gunye, Phys. Rev. **155**, 1084 (1967); M. R. Gunye and C. S. Warke, *ibid.* **156**, 1087 (1967); **159**, 885 (1967); **164**, 1264 (1967).
[9] S. K. Khosa and P. K. Mattu, Phys. Rev. C **43**, 634 (1991).
[10] A. J. Singh, P. K. Raina, and S. K. Dhima, Phys. Rev. C **50**, 2307 (1994).
[11] E. Wust, A. Ansari, and U. Mosel, Nucl. Phys. **A435**, 477 (1985).
[12] P. N. Tripathi and S. K. Sharma, Phys. Rev. C **34**, 1081 (1986).
[13] J. Y. Zeng and T. S. Cheng, Nucl. Phys. **A405**, 1 (1983).
[14] J. Y. Zeng, T. S. Cheng, L. Cheng, and C. S. Wu, Nucl. Phys. **A411**, 49 (1983); **A414**, 253 (1984); **A421**, 125 (1984).
[15] C. S. Wu and J. Y. Zeng, Phys. Rev. C **40**, 998 (1989); **41**, 1822 (1990).
[16] C. S. Wu and J. Y. Zeng, Phys. Rev. Lett. **66**, 1022 (1991).
[17] J. Y. Zeng, Y. A. Lei, T. H. Jin, and Z. J. Zhao, Phys. Rev. C **50**, 746 (1994).
[18] J. Y. Zeng, T. H. Jin, and Z. J. Zhao, Phys. Rev. C **50**, 1388 (1994).
[19] P. W. M. Glaudemans, P. J. Brussaard, and B. H. Wildenthal, Nucl. Phys. **A102**, 593 (1967).
[20] P. J. Brussaard and P. W. M. Glaudemans, *Shell-Model Applications in Nuclear Spectroscopy* (North-Holland, Amsterdam, 1977), Chap. 6.
[21] I. Kelson, Phys. Rev. **132**, 2189 (1963).
[22] J. C. Parikh and J. P. Svenne, Phys. Rev. **174**, 1343 (1968).
[23] Y. Han, High Energy Phys. Nucl. Phys. **22**, 1020 (1998).
[24] D. E. Alburger, Nucl. Data Sheets **49**, 237 (1986).
[25] L. K. Peker, Nucl. Data Sheets **68**, 271 (1993).
[26] S. Raman, C. H. Malarkey, W. T. Milner, C. W. Nestor, Jr., and P. H. Stelson, At. Data Nucl. Data Tables **36**, 1 (1987).
[27] N. R. F. Rammo, P. J. Nolan, L. L. Green, A. N. James, J. F. Sharpey-Schafer, and H. M. Sheppard, J. Phys. G **8**, 101 (1982).
[28] K. W. Schmid, F. Grummer, and A. Faessler, Phys. Rev. C **29**, 308 (1984).
[29] D. E. Alburger, Nucl. Data Sheets **45**, 557 (1985).
[30] T. W. Burrows, Nucl. Data Sheets **68**, 1 (1993).